

Vacuum currents in curved tubes

A. A. Saharian

*Institute of Physics, Yerevan State University,
1 Alex Manogian Street, 0025 Yerevan, Armenia*

May 15, 2024

Abstract

We investigate the combined effects of spatial curvature and topology on the properties of the vacuum state for a charged scalar field localized on rotationally symmetric 2D curved tubes. For a general spatial geometry and for quasiperiodicity condition with a general phase, the representation of the Hadamard function is provided where the topological contribution is explicitly extracted. As an important local characteristic of the vacuum state the expectation value of the current density is studied. The vacuum current is a periodic function of the magnetic flux enclosed by the tube with the period of flux quantum. The general formula is specified for constant radius and conical tubes. As another application, we consider the Hadamard function and the vacuum current density for a scalar field on the Beltrami pseudosphere. Several representations are provided for the corresponding expectation value. For small values of the proper radius of the tube, compared with the curvature radius, the effect of spatial curvature on the vacuum current is weak and the leading term in the corresponding expansion coincides with the current density on a constant radius tube. The effect of curvature is essential for proper radii of the tube larger than the radius of spatial curvature. In this limit the fall-off of the current density, as a function of the proper radius, follows a power-law for both massless and massive fields. This behavior is in clear contrast to the one for a constant radius tube with exponential decay for massive fields. We also compare the vacuum currents on the Beltrami pseudosphere and on locally de Sitter and anti-de Sitter 2D tubes.

Keywords: vacuum currents; nontrivial topology; emergent gravity; Beltrami pseudosphere

1 Introduction

The canonical quantization of fields is based on the expansion of the field operator in terms of a complete set of mode functions being the solutions of the classical field equation. The coefficients of the expansion determine the annihilation and creation operators that are used for the construction of the Fock space of states started from the vacuum state. The latter is defined as the state of quantum field nullified by the action of the annihilation operator. The mode functions are sensitive to both local and global characteristics of the background space-time and the same is the case for the properties of the vacuum and particle states. Among the interesting areas of research in quantum field theory is the dependence of those properties on the geometry and topology of the background spacetime. The corresponding effects play an important role in gravity, cosmology, in physical models with extra compact dimensions, in condensed matter physics and in finite temperature field theory (see, for example, [1, 2, 3]). As an example of the combined influence of the spatial curvature and topology on the properties of quantum vacuum, in the present paper we consider the generation of vacuum currents for a scalar field localized on 2D curved tubes. These currents have common roots with persistent currents in mesoscopic rings, widely studied in the literature for different physical systems (see, e.g., [4, 5, 6, 7] and references therein). The experimental detection of persistent currents in normal metal rings has been reported in [8, 9].

The investigation of field theoretical effects in (2+1)-dimensional spacetimes has attracted a great deal of attention. The interest is motivated by several reasons. In addition to be simplified toy models of (3+1)-dimensional physics, the change in the number of spatial dimension leads to new types of phenomena. They include new mechanisms for symmetry breaking, parity violation, and fractionalization of quantum numbers. From the fundamental point of view, an important aspect in 2D gauge theories is the mechanism that generates a topological mass for gauge bosons without breaking the gauge symmetry [10]. 2D models also appear as effective field theories describing the physics of compact subspace in Kaluza-Klein and braneworld type theories with extra dimensions. The recent advances in synthesis methods and techniques for planar condensed matter systems (2D materials) have increased significantly the interest to 2D physics. The long-wavelength degrees of freedom in a number of those systems is described by 2D relativistic field theory. Well known examples are the graphene family materials with the low-energy excitations of the electronic subsystem described by 2D Dirac equation involving the Fermi velocity instead of light velocity (see, e.g., [11, 12]).

In the physics of 2D materials the topological issues play an important role both in the space of states and in the coordinate space. In particular, topological phases of matter and topological defects are currently the subject of active research. Here we will investigate the influence of spatial topology and curvature on the ground state properties of the 2D scalar field. As the representative of those properties the current density is taken. The simplest example of nontrivial topology is a cylindrical tube with constant radius. The vacuum currents in that geometry for scalar and Dirac fields have been investigated in [13, 14] as special cases of more general geometries with an arbitrary number of spatial dimensions and with toroidally compactified subspace. Both cases of infinite and finite length tubes were considered. The corresponding finite temperature charge and current densities have been discussed in [15, 16]. The vacuum currents induced by magnetic fluxes in conical geometries, describing idealized cosmic strings, are considered in [17, 18, 19, 20]. More realistic geometry of a finite thickness cosmic string with a cylindrically symmetric core is discussed in [21]. The compactification of cosmic strings along the axial direction may lead to the component of the current density along that direction [22, 23]. The ground state charge and current densities for a fermionic field on a two-dimensional circular ring were studied in [24].

The geometric curvature of 2D materials provides an additional mechanism to control their physical characteristics and opens new perspectives for applications. Among the interesting features is the generation of effective gauge fields [25, 26]. The investigation of the curvature induced effects in those systems is also important from the point of view of fundamental physics giving insights on the influence of gravitational field on quantum matter. Motivated by these technological and fundamental perspectives, the effects of curvature in 2D physics are in the focus of active research (see, for example, [27]-[53], covering various aspects of the topic). Related to the topic of the present paper, the vacuum expectation value of the current density for scalar and fermionic fields in locally de Sitter (dS) and anti-de Sitter (AdS) spacetimes with toroidal subspaces is investigated in [54, 55] (for a review see [7]).

The paper is organized as follows. In the next section we describe the background geometry and present some special cases. The scalar field modes and the Hadamard function for a general rotationally symmetric tube are given in Section 3. By using the Hadamard function, the vacuum expectation value of the current density is investigated in Section 4. The vacuum currents for some special cases of the tube geometry are presented in Section 5. As an application of general formulas, in Section 6 we investigate the expectation value of the current density on the Beltrami pseudosphere. The asymptotic analysis and numerical results are presented. The main results of the are summarized in Section 7. In Appendix A the expressions for the current densities in (2+1)-dimensional locally dS and AdS spacetimes with a spatial dimension compactified to a circle are presented.

2 Geometry of the problem and special cases

2.1 Background geometry and induced metric

We consider a cylindrical surface in a 3-dimensional Euclidean space with coordinates $X^i = (X, Y, Z)$, $i = 1, 2, 3$. The equation of the surface in the parametric form is expressed as

$$X = f(u) \cos \phi, \quad Y = f(u) \sin \phi, \quad Z = z(u), \quad (2.1)$$

where ϕ is the angular coordinate, $0 \leq \phi \leq 2\pi$. The radius of the surface for a fixed Z is given by the function $f(u) = \sqrt{X^2 + Y^2}$ (see Fig. 1). In the corresponding (3+1)-dimensional Minkowski spacetime the line element has the form $ds_4^2 = \eta_{\mu\nu} dX^\mu dX^\nu$, where $\eta_{\mu\nu}$ is the Minkowskian metric tensor. We will denote the spacetime coordinates on the cylindrical surface by $x^i = (x^0 = t = X^0, x^1 = u, x^2 = \phi)$. For the line element on the surface one has $ds^2 = g_{ik} dx^i dx^k$, where the components of the induced metric $g_{ik} = \eta_{\mu\nu} \partial_i X^\mu \partial_k X^\nu$ are given by

$$g_{00} = 1, \quad g_{11} = -[f'^2(u) + z'^2(u)], \quad g_{22} = -f^2(u), \quad (2.2)$$

and the off-diagonal components vanish. Here the prime stands for the derivative of the function with respect to the argument.

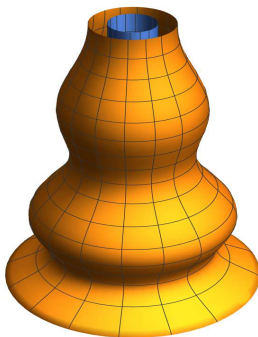


Figure 1: Curved tube threaded by a magnetic flux.

The metric tensor can be further simplified introducing a new coordinate w in accordance with

$$w = w(u) = \int_{u_0}^u du \sqrt{f'^2(u) + z'^2(u)}. \quad (2.3)$$

In terms of this coordinate the line element on the cylinder is written as

$$ds^2 = dt^2 - dw^2 - p^2(w) d\phi^2, \quad (2.4)$$

where the function $p(w)$ is defined by the relation $p(w) = f(u(w))$, with $u = u(w)$ determined from (2.3). By taking into account that $p'(w) = 1/\sqrt{1 + z'^2(u)/f'^2(u)}$, for the function $h(w) = z(u(w))$ one gets

$$h(w) = \pm \int_{w_0}^w dw \sqrt{1 - p'^2(w)}, \quad (2.5)$$

with w_0 being a constant. In terms of w the equation of the surface in the parametric form is rewritten as

$$X = p(w) \cos \phi, \quad Y = p(w) \sin \phi, \quad Z = h(w), \quad (2.6)$$

where the function $h(w)$ is defined by (2.5). In coordinates (t, w, ϕ) , the nonzero components of the Ricci tensor and the Ricci scalar for a (2+1)-dimensional spacetime determined by (2.4) have the form

$$R_1^1 = R_2^2 = -\frac{p''(w)}{p(w)}, \quad R = -2\frac{p''(w)}{p(w)}. \quad (2.7)$$

The radius of the tube for a fixed w is given by $p(w)$ and for the length of compact dimension we have $2\pi p(w)$.

2.2 Special cases

Let us consider some special cases of the general geometry described above. The simplest one corresponds to a cylinder with constant radius L . In this case one has

$$p(w) = L \quad (2.8)$$

and $-\infty < w < +\infty$. The second example is described by a linear function

$$p(w) = \alpha w, \quad \alpha = \text{const.} \quad (2.9)$$

Assuming $\alpha < 1$, for the function $h(w)$ from (2.5) one finds

$$h(w) = \sqrt{1 - \alpha^2 w}. \quad (2.10)$$

where we have taken $w_0 = 0$. The line element takes the form

$$ds^2 = dt^2 - dw^2 - \alpha^2 w^2 d\phi^2, \quad (2.11)$$

with $0 \leq w < \infty$. For $\alpha = 1$ this is the line element on a plane in polar coordinates. For $\alpha < 1$ it describes a cone with an opening angle $2\pi\alpha$. It is obtained from a plane cutting the angle $2\pi(1 - \alpha)$ and gluing the edges of the remaining angle. For a given coordinate $Z = h(w)$ in the embedding space the radius of the circle is given by (2.9). The tip of the cone is located at $(X, Y, Z) = (0, 0, 0)$. Note that for $w \neq 0$ one has $R_{ik} = 0$ and both the spacetime and space are flat. The graphitic cones are among the possible condensed matter realizations of 2D conical geometry. The corresponding values of the parameter α are determined by the structure of the graphene hexagonal lattice and are given by $\alpha = 1 - N_c/6$ with $N_c = 1, 2, 3, 4, 5$. Graphitic cones with all those values of the parameter α have been observed in experiments (see, e.g., [56, 57]).

As the next example we consider a constant curvature space with

$$\frac{p''(w)}{p(w)} = \pm \frac{1}{a^2} = \text{const.} \quad (2.12)$$

For the corresponding Gaussian curvature one has $K = R/2 = \mp 1/a^2$. In the case of a constant positive curvature space (lower sign in (2.12)) the solution can be taken in the form

$$p(w) = L \sin(w/a), \quad 0 \leq w/a \leq \pi. \quad (2.13)$$

Introducing the angular coordinate $\theta = w/a$, $0 \leq \theta \leq \pi$, the line element is written as

$$ds^2 = dt^2 - a^2 (d\theta^2 + \sin^2 \theta d\phi^2). \quad (2.14)$$

This corresponds to a sphere with radius a . The condensed matter realizations of this geometry include fullerenes and topological insulators with spherical surfaces [27, 28, 32, 36]. In the long-wavelength approximation the dynamics of the corresponding electronic subsystem is described by the 2D Dirac equation with a sphere as a background space.

For a negative curvature space (the upper sign) one gets the equation

$$p''(w) = p(w)/a^2. \quad (2.15)$$

Three separate subcases are realized. For the first one we take the solution of (2.15) given by

$$p(w) = Le^{w/a}, \quad -\infty < w < +\infty, \quad (2.16)$$

where L is a constant with dimension of length. For the line element on the tube one gets

$$ds^2 = dt^2 - dw^2 - L^2 e^{2w/a} d\phi^2. \quad (2.17)$$

The spatial geometry described by this element corresponds to the Beltrami pseudosphere. The coordinates of the embedding space are given by (2.6). For the corresponding part of the surface we have $p'(w) \leq 1$. This shows that though in (2.16) one has $-\infty < w < +\infty$, only the part of the space corresponding to

$$w \leq w_b \equiv -a \ln(L/a), \quad (2.18)$$

can be embedded in a 3-dimensional Euclidean space. For the function $h(w)$ in the embedding space (with the upper sign in (2.5)) one gets

$$h(w) = a \left[\sqrt{1 - e^{2(w-w_b)/a}} - \operatorname{arctanh} \left(\sqrt{1 - e^{2(w-w_b)/a}} \right) \right]. \quad (2.19)$$

On the left panel of Fig. 1 we have presented the spatial geometry corresponding to (2.17) as a surface (2.6) in an Euclidean space with coordinates (X, Y, Z) .

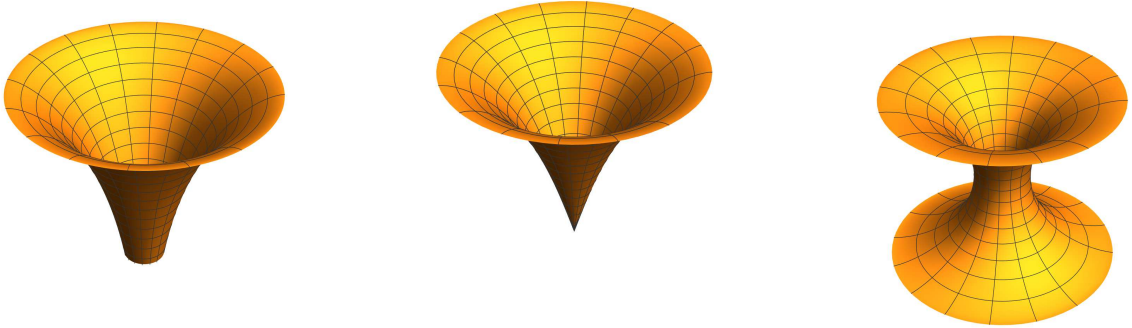


Figure 2: The Beltrami (left), elliptic (middle) and hyperbolic (right) pseudospheres embedded in a 3-dimensional Euclidean space.

For the second subcase of the negative curvature space we take

$$p(w) = L \sinh(w/a), \quad 0 \leq w < \infty, \quad (2.20)$$

with the line element

$$ds^2 = dt^2 - dw^2 - L^2 \sinh^2(w/a) d\phi^2. \quad (2.21)$$

The spatial geometry corresponds to the elliptic pseudosphere. For the part embedded in a 3-dimensional Euclidean space one finds

$$0 \leq w \leq w_{be} \equiv a \operatorname{arccosh}(a/L), \quad (2.22)$$

with $L/a \leq 1$ and the function $h(w)$ in (2.6) is given by

$$h(w) = a \int_0^{w/a} dx \sqrt{1 - (L/a)^2 \cosh^2 x}. \quad (2.23)$$

The integral in the right-hand side is expressed in terms of the elliptic functions. The middle panel in Fig. 2 presents the part of the elliptic pseudosphere embedded in an Euclidean space.

The third subcase for the negative curvature space corresponds to the function

$$p(w) = L \cosh(w/a), \quad -\infty < w < \infty, \quad (2.24)$$

and the line element is given by

$$ds^2 = dt^2 - dw^2 - L^2 \cosh^2(w/a) d\phi^2. \quad (2.25)$$

This correspond to the hyperbolic pseudosphere. For the piece of the geometry embedded in a Euclidean space we have

$$-w_{\text{bh}} \leq w \leq w_{\text{bh}} \equiv a \operatorname{arcsinh}(a/L). \quad (2.26)$$

The function $h(w)$ is determined from

$$h(w) = a \int_0^{w/a} dx \sqrt{1 - (L/a)^2 \sinh^2 x}. \quad (2.27)$$

Similar to the previous case this integral is expressed in terms of the elliptic functions. On the right panel of Fig. 2 we display the part of the hyperbolic pseudosphere embedded in Euclidean space in accordance with (2.6).

The condensed matter realizations of negative constant curvature surfaces by 2D materials have been discussed by several authors. In particular, those structures have been used as simplified models for 2D black holes and wormholes (see, for example, [33, 34, 35, 37, 41, 44, 45, 46, 49, 50, 51] and references therein). One can get new kinds of structures combining different geometries discussed above. For example, cylindrical and planar geometries have been combined to construct simplified models for 2D wormholes. The combination of spherical and cylindrical geometries is realized in capped graphene nanotubes. The vacuum expectation values of the field squared and of the energy-momentum tensor for a massive scalar field in the latter geometry have been studied in [58].

3 Scalar field modes and the Hadamard function

Having specified the geometry we turn to the field. We consider a complex scalar field $\varphi(x)$ localized on a cylindrical surface. The corresponding field equation reads

$$\left(g^{ik} D_i D_k + m^2 + \xi R \right) \varphi(x) = 0, \quad D_k = \nabla_k + ieA_k, \quad (3.1)$$

where A_i is the vector potential for a classical gauge field, ξ is the curvature coupling parameter and ∇_k is the covariant derivative operator corresponding to the metric tensor g^{ik} determined by (2.4). In the special cases of minimally and conformally coupled scalar fields one has $\xi = 0$ and $\xi = 1/8$, respectively. The complex scalar field describes charged excitations in Bose-Einstein condensates, phononic degrees of freedom and surface plasmons (see [59, 60, 61] for some recent references). We consider a background with nontrivial topology and the periodicity condition along the direction of the angular coordinate ϕ needs to be specified. We will impose a quasiperiodicity condition

$$\varphi(t, w, \phi + 2\pi) = e^{i\tilde{\alpha}_p} \varphi(t, w, \phi), \quad (3.2)$$

with a constant phase $\tilde{\alpha}_p$. For the gauge field a simple configuration will be considered with $A_k = (0, 0, A_2 = \text{const})$ in the spacetime coordinates (t, w, ϕ) . This corresponds to a magnetic flux $\Phi = -2\pi A_2$ in the embedding space, threading the tube. On the tube, the field tensor for the gauge field is zero and the effect on the properties of 2D quantum scalar field is of the Aharonov-Bohm type. The gauge field under consideration is excluded from the field equation by the gauge transformation $\varphi'(x) = e^{ie\kappa(x)}\varphi(x)$, $A'_k = A_k - \partial_k\kappa(x)$ with the function $\kappa(x) = A_2\phi$. In the new gauge $A'_k = 0$ and the scalar field obeys the periodicity condition

$$\varphi'(t, w, \phi + 2\pi) = e^{i\alpha_p}\varphi'(t, w, \phi), \quad \alpha_p = \tilde{\alpha}_p + 2\pi e A_2. \quad (3.3)$$

The phase shift in this condition is presented as $2\pi e A_2 = -2\pi\Phi/\Phi_0$, where $\Phi_0 = 2\pi/e$ is the flux quantum. The discussion below will be presented in terms of the field $\varphi'(x)$ omitting the prime.

The properties of the vacuum state $|0\rangle$ for the field $\varphi(x)$ are contained in two-point functions describing the correlations of the vacuum fluctuations in different spacetime points. For the evaluation of two-point functions we need to have the complete set of positive and negative energy scalar modes $\{\varphi_\sigma^{(+)}(x), \varphi_\sigma^{(-)}(x)\}$ obeying the field equation (3.1) with $A_k = 0$ and the condition (3.3). Here, σ stands for the set of quantum numbers specifying the modes. For the geometry described by (2.4) the mode functions are presented in the form

$$\varphi_\sigma^{(\pm)}(x) = e^{ik_n\phi \mp i\omega t} z_\sigma(w), \quad k_n = n + \frac{\alpha_p}{2\pi}, \quad n = 0, \pm 1, \pm 2, \dots, \quad (3.4)$$

where the eigenvalues of the momentum k_n along the azimuthal direction are determined by the condition (3.3). Substituting into (3.1), the following equation is obtained for the function $z_\sigma(w)$:

$$\frac{[p(w)z'_\sigma(w)]'}{p(w)} + \left[2\xi \frac{p''(w)}{p(w)} - \frac{u^2}{p^2(w)} + \lambda^2 \right] z_\sigma(w) = 0, \quad (3.5)$$

where $\lambda^2 = \omega^2 - m^2$, $u = k_n$. We denote by k_w the quantum number related to the w -direction. The parameter λ and the energy $\omega = \sqrt{\lambda^2 + m^2}$ depend on that quantum number. For some geometries it will be convenient to take λ in the role of the quantum number k_w . The mode functions are specified by the set of quantum numbers $\sigma = (k_w, k_n)$ and $z_\sigma(w) = z_{k_w, k_n}(w)$. The normalization condition for the modes has the form

$$\int dw \int_0^{2\pi} d\phi \sqrt{|g|} \varphi_\sigma^{(\pm)}(x) \varphi_{\sigma'}^{(\pm)*}(x) = \frac{\delta_{nn'}}{2\omega} \delta_{k_w k'_w}. \quad (3.6)$$

Here, $\delta_{k_w k'_w}$ is understood as the Kronecker delta for discrete quantum number k_w and as the Dirac delta function $\delta(k_w - k'_w)$ for continuous one. Substituting (3.4) in (3.6), we get the orthonormalization condition for the function $z_{k_w, k_n}(w)$:

$$\int dw p(w) z_{k_w, k_n}(w) z_{k'_w, k'_n}^*(w) = \frac{\delta_{k_w k'_w}}{4\pi\omega}, \quad (3.7)$$

where the limits of the integration are determined by the range of variation of the coordinates w and depend on the specific problem (see examples below).

Having the complete set of mode functions we can evaluate the Hadamard function, defined as the vacuum expectation value (VEV)

$$G(x, x') = \langle 0 | \varphi(x) \varphi^\dagger(x') + \varphi^\dagger(x') \varphi(x) | 0 \rangle, \quad (3.8)$$

where the dagger stands for the hermitian conjugate. Expanding the field operator in terms of the complete set $\{\varphi_\sigma^{(+)}, \varphi_\sigma^{(-)}\}$, the following mode sum formula is obtained:

$$G(x, x') = \sum_\sigma \sum_{s=+,-} \varphi_\sigma^{(s)}(x) \varphi_\sigma^{(s)*}(x'), \quad (3.9)$$

where \sum_σ includes the summation over the discrete components of the collective index σ and the integration over the continuous ones. Substituting the modes (3.4) we get

$$G(x, x') = 2 \sum_{n=-\infty}^{+\infty} e^{ik_n \Delta \phi} \sum_{k_w} z_{k_w, k_n}(w) z_{k_w, k_n}^*(w') \cos(\omega \Delta t), \quad (3.10)$$

with $\Delta \phi = \phi - \phi'$, $\Delta t = t - t'$, $\omega = \sqrt{\lambda^2 + m^2}$, and $\lambda = \lambda(k_w)$. The symbol \sum_{k_w} is understood as summation for discrete quantum number k_w and integration over k_w for the continuous one.

In order to see the effects of the compactification, it is of interest to compare the function $G(x, x')$ with the corresponding function in the geometry where the coordinate ϕ is not compactified, $-\infty < \phi < +\infty$. The line element is still given by (2.4). Now the mode functions have the form

$$\varphi_{0\sigma}^{(\pm)} = e^{iu\phi \mp i\omega t} z_{k_w, u}^{(0)}(w), \quad -\infty < u < +\infty, \quad (3.11)$$

with $\sigma = (k_w, u)$. The function $z_{k_w, u}^{(0)}(w)$ obeys the equation (3.5). From the corresponding normalization condition one gets

$$\int dw p(w) z_{k_w, u}^{(0)}(w) z_{k'_w, u}^{(0)*}(w) = \frac{\delta_{k_w k'_w}}{4\pi\omega}, \quad (3.12)$$

which is the same as in (3.7). The corresponding Hadamard function is presented in the form

$$G_0(x, x') = 2 \int_{-\infty}^{+\infty} du e^{iu\Delta\phi} \sum_{k_w} z_{k_w, u}^{(0)}(w) z_{k_w, u}^{(0)*}(w') \cos(\omega \Delta t), \quad (3.13)$$

again with $\omega = \sqrt{\lambda^2 + m^2}$.

In the equation (3.5) for $z_\sigma(w)$ the parameter $u = k_n$ appears in the form k_n^2 and it can be assumed that $z_\sigma(w) = z_{k_w, k_n}(w) = z_{k_w}(w, |k_n|)$. We apply to the sum over n in (3.10) the summation formula [14]

$$\sum_{n=-\infty}^{+\infty} g(k_n) f(|k_n|) = \int_0^\infty du [g(u) + g(-u)] f(u) + i \int_0^\infty du [f(iu) - f(-iu)] \sum_{s=\pm 1} \frac{g(isu)}{e^{2\pi u + is\alpha_p} - 1}. \quad (3.14)$$

with $g(u) = e^{iu\Delta\phi}$ and

$$f(u) = z_{k_w}(w, u) z_{k_w}^*(w', u). \quad (3.15)$$

It is worth mentioning that the complex conjugate in (3.15) is taken for real values of u and then the result is analytically continued in the complex plane. We will assume that the function obtained in this way is analytic in the right half-plane. The part with the first term in the right-hand side gives the Hadamard function (3.13) and we get

$$\begin{aligned} G(x, x') &= G_0(x, x') + 2i \sum_{k_w} \cos(\omega \Delta t) \int_0^\infty du \sum_{s=\pm 1} \frac{e^{-su\Delta\phi}}{e^{2\pi u + is\alpha_p} - 1} \\ &\quad \times [z_{k_w}(w, iu) z_{k_w}^*(w', iu) - z_{k_w}(w, -iu) z_{k_w}^*(w', -iu)]. \end{aligned} \quad (3.16)$$

Note that

$$\sum_{s=\pm 1} \frac{e^{-su\Delta\phi}}{e^{2\pi u + is\alpha_p} - 1} = \frac{2e^{2\pi u} \cosh(2\pi\Delta\phi + i\alpha_p) - 2 \cosh(u\Delta\phi)}{e^{4\pi u} - 2e^{2\pi u} \cos \alpha_p + 1}. \quad (3.17)$$

Again, it should be noted that in (3.16) the functions $z_{k_w}^*(w', \pm iu)$ are understood as the following: we first consider the function $z_{k_w}^*(w', u)$ for real u and then replace u by $\pm iu$. Examples of the function $p(w)$ for which the solution $z_{k_w}(w, u)$ is expressed in terms of the known functions are given in Section 5.

The function $z_\sigma(w) = z_{k_w}(w, u)$ in (3.16) obeys the equation (3.5). From here it follows that for any two solutions $z_{(1)k_w}(w, u)$ and $z_{(2)k_w}(w, u)$ of (3.5) the following Wronskian relation takes place

$$z_{(1)k_w}(w, u)\partial_w z_{(2)k_w}(w, u) - z_{(2)k_w}(w, u)\partial_w z_{(1)k_w}(w, u) = \frac{C}{p(w)}, \quad (3.18)$$

with a constant C which may depend on k_w and u . This relation is valid for general u , including the complex values.

The representation (3.16) separates explicitly the contribution in the Hadamard function induced by the compactification of the coordinate ϕ . The local geometry for the compactified and decompactified spaces is the same and, hence, the corresponding divergences in the coincidence limit $x' \rightarrow x$ are the same as well. From here it follows that in the evaluation of the VEVs for local physical observables, bilinear in the field operator, the renormalization is required for the parts coming from the function $G_0(x, x')$. The renormalized topological contributions in the VEVs are directly obtained from the second term in the right-hand side of (3.16) or from its derivatives taking the coincidence limit. In the next section this will be illustrated for the current density.

4 VEV of the current density

Given the Hadamard function, the VEVs of physical observables bilinear in the field can be evaluated. As an important characteristic of the vacuum state here we consider the VEV of the current density $\langle 0|j_k(x)|0\rangle \equiv \langle j_k(x)\rangle$, where the corresponding operator is given by

$$j_k(x) = ie[\varphi^\dagger(x)\partial_k\varphi(x) - (\partial_k\varphi(x))^\dagger\varphi(x)]. \quad (4.1)$$

The VEV is expressed in terms of the Hadamard function as

$$\langle j_k(x)\rangle = \frac{i}{2}e \lim_{x' \rightarrow x} (\partial_k - \partial'_k)G(x, x'). \quad (4.2)$$

With the Hadamard function from (3.16), we see that the charge density vanishes, $\langle j_0\rangle = 0$.

For the contravariant component of the current density along the w -direction, $\langle j^1\rangle = -\langle j_1\rangle$, we get

$$\langle j^1\rangle = \langle j^1\rangle_0 + \frac{ie}{p(w)} \sum_{k_w} \int_0^\infty du \sum_{s=\pm 1} \frac{C_{k_w}(iu) - C_{k_w}(-iu)}{e^{2\pi u + is\alpha_p} - 1}, \quad (4.3)$$

where

$$\langle j^1\rangle_0 = \frac{e}{p(w)} \sum_{k_w} \int_{-\infty}^{+\infty} du C_{k_w}(u) \quad (4.4)$$

is the current density in the geometry where the coordinate ϕ is not compactified. Here, the function $C_{k_w}(u)$ for real u is defined in accordance with

$$z_{k_w}^*(w, u)\partial_w z_{k_w}(w, u) - z_{k_w}(w, u)\partial_w z_{k_w}^*(w, u) = \frac{iC_{k_w}(u)}{p(w)}. \quad (4.5)$$

For real u the function $C_{k_w}(u)$ is real. As it has been emphasized above, the renormalization is required only for the part $\langle j^1\rangle_0$.

By using (3.16) and (4.2), for the physical component of the azimuthal current density, $\langle j^\phi\rangle = p(w)\langle j^2\rangle = -\langle j_2\rangle/p(w)$, one finds

$$\langle j^\phi\rangle = -\frac{2e}{p(w)} \sum_{k_w} \int_0^\infty du u \sum_{s=\pm 1} s \frac{z_{k_w}(w, iu)z_{k_w}^*(w, iu) - z_{k_w}(w, -iu)z_{k_w}^*(w, -iu)}{e^{2\pi u + is\alpha_p} - 1}. \quad (4.6)$$

The azimuthal current vanishes in the geometry with uncompactified ϕ and the current (4.6) is induced by the compactification. The component $\langle j^1 \rangle$ is an even function of α_p and the component $\langle j^\phi \rangle$ is an odd function. An alternative expression is obtained from (4.6) by using the expansion $1/(e^y - 1) = \sum_{l=1}^{\infty} e^{-ly}$:

$$\langle j^\phi \rangle = \frac{4ie}{p(w)} \sum_{l=1}^{\infty} \sin(l\alpha_p) \sum_{k_w} \int_0^{\infty} du u e^{-2\pi l u} [z_{k_w}(w, iu) z_{k_w}^*(w, iu) - z_{k_w}(w, -iu) z_{k_w}^*(w, -iu)]. \quad (4.7)$$

This current is an odd periodic function of the magnetic flux, enclosed by the tube, with the period of flux quantum.

5 Vacuum currents in special cases

As applications of the general results given above, in this section we consider special cases.

5.1 Cylinder with a constant radius

For a cylinder with a constant radius L the mode functions have the form

$$z_\sigma(w) = z_{k_w}(w, |k_n|) = \frac{e^{ik_w w}}{\sqrt{8\pi^2 L \omega}}, \quad -\infty < k_w < +\infty, \quad (5.1)$$

with $\omega = \sqrt{k_w^2 + k_n^2/L^2 + m^2}$. Substituting in (3.10) with $\sum_{k_w} \rightarrow \int_{-\infty}^{+\infty} dk_w$ and integrating over k_w , we get

$$G(x, x') = \frac{1}{2\pi^2 L} \sum_{n=-\infty}^{+\infty} e^{ik_n \Delta\phi} K_0 \left(\sqrt{k_n^2/L^2 + m^2} \sqrt{(\Delta w)^2 - (\Delta t)^2} \right), \quad (5.2)$$

where $K_\nu(x)$ is the Macdonald function [62]. For the function $C_{k_w}(u)$ defined by (4.5) one has $C_{k_w}(u) = k_w/(4\pi^2 \omega)$. It is an odd function of k_w and the integration over k_w gives a zero current along the w -direction, $\langle j^1 \rangle = 0$. For the azimuthal current density from (4.7) we find

$$\langle j^\phi \rangle = \frac{e}{4\pi^3 L^2} \sum_{l=1}^{\infty} \frac{1 + 2\pi l L m}{l^2 e^{2\pi l L m}} \sin(l\alpha_p). \quad (5.3)$$

This result is the special case of the general formula from [15].

5.2 Current density on a cone

In the case of a cone with an opening angle $2\pi\alpha$ the function $p(w)$ is given by (2.9). As a quantum number k_w we take $k_w = \lambda$. The general solution of the equation (3.5) is a linear combination of the Bessel and Neumann functions $J_{|k_n|/\alpha}(\lambda w)$ and $Y_{|k_n|/\alpha}(\lambda w)$. For $|n| \geq 2$, from the normalizability condition it follows that the function $J_{|k_n|/\alpha}(\lambda w)$ should be taken. For the modes with $|n| = 1$, under the condition $1 - |\alpha_p|/2\pi < \alpha$, and for $n = 0$, under the condition $|\alpha_p| < 2\pi\alpha$, the irregular part with the function $Y_{|k_n|/\alpha}(\lambda w)$ may also be present. In those cases, in order to uniquely define the mode functions, an additional boundary condition is required on the cone apex. Here we will consider a special case where the function

$$z_{k_w}(w, |k_n|) = c_1 J_{|k_n|/\alpha}(\lambda w), \quad 0 \leq k_w = \lambda < \infty \quad (5.4)$$

is taken for all values of n . By using the integral

$$\int_0^{\infty} dw w J_{|k_n|/\alpha}(\lambda w) J_{|k_n|/\alpha}(\lambda' w) = \frac{1}{\lambda} \delta(\lambda - \lambda'), \quad (5.5)$$

from (3.7) for the normalization coefficient one gets $c_1 = \sqrt{\lambda/(4\pi\alpha\omega)}$. With this coefficient, the function $z_{k_w}(w, u)$ in (4.5) is real and, hence, $C_{k_w}(u) = 0$. This shows that $\langle j^1 \rangle = \langle j^1 \rangle_0 = 0$ for the current density in the axial direction.

Substituting the functions (5.4) in (4.6), for the VEV of the azimuthal current we find

$$\langle j^\phi \rangle = \frac{2e}{\pi w} \int_0^\infty d\lambda \frac{\lambda}{\sqrt{\lambda^2 + m^2}} \int_0^\infty du u \operatorname{Im} \left(\frac{1}{e^{2\pi\alpha u + i\alpha_p} - 1} \right) \operatorname{Im} [J_{iu}^2(\lambda w)], \quad (5.6)$$

where the integration variable is redefined as $u/\alpha \rightarrow u$. For the further transformation we employ the integral representation

$$\frac{1}{\sqrt{\lambda^2 + m^2}} = \frac{2}{\sqrt{\pi}} \int_0^\infty d\tau e^{-\tau^2(\lambda^2 + m^2)}. \quad (5.7)$$

With this representation, the integral over λ in (5.6) is evaluated by using the formula from [63]. This gives

$$\int_0^\infty d\lambda \lambda e^{-\tau^2 \lambda^2} \operatorname{Im} [J_{iu}^2(\lambda w)] = -\frac{\sinh(\pi u)}{2\pi\tau^2} e^{-x} K_{iu}(x), \quad (5.8)$$

with $x = w^2/(2\tau^2)$. Passing from τ to a new integration variable x one gets

$$\langle j^\phi \rangle = \frac{e \sin \alpha_p}{\sqrt{2\pi^{5/2} w^2}} \int_0^\infty \frac{dx}{\sqrt{x}} e^{-x - w^2 m^2 / 2x} \int_0^\infty du \frac{u \sinh(\pi u) K_{iu}(x)}{\cosh(2\alpha u) - \cos \alpha_p}, \quad (5.9)$$

where we have used

$$\operatorname{Im} \left(\frac{1}{e^{2\alpha u + i\alpha_p} - 1} \right) = -\frac{1}{2} \frac{\sin \alpha_p}{\cosh(2\alpha u) - \cos \alpha_p}. \quad (5.10)$$

An alternative expression for the current density in general number of spatial dimensions D is given in [21]. Specified for the case $D = 2$ it has the form

$$\begin{aligned} \langle j^\phi \rangle &= \frac{ewm^3}{\pi} \left[\sum_{n=1}^{[1/2\alpha]} \sin(n\alpha_p) \sin(2\pi n\alpha) g(2mw \sin(\pi n\alpha)) \right. \\ &\quad \left. + \frac{1}{2\pi\alpha} \int_0^\infty dy f(\alpha, \alpha_p, y) \frac{g(2mw \cosh(y/2)) \sinh y}{\cosh(y/\alpha) - \cos(\pi/\alpha)} \right], \end{aligned} \quad (5.11)$$

where $[1/2\alpha]$ stands for the integer part of $1/2\alpha$, $g(x) = (1+x)e^{-x}/x^3$ and

$$f(\alpha, \alpha_p, y) = \sin(\alpha_p/2\alpha) \sinh[(1 - \alpha_p/2\pi)y/\alpha] - \sin[\pi(1 - \alpha_p/2\pi)/\alpha] \sinh(\alpha_p y/2\pi\alpha). \quad (5.12)$$

For $\alpha > 1/2$ the first term in the square brackets of (5.11) is absent.

The formula (5.9) is further simplified for a massless field by using the integration formula [63]

$$\int_0^\infty \frac{dx}{\sqrt{x}} e^{-x} K_{iu}(x) = \sqrt{\frac{\pi}{2}} \frac{\pi}{\cosh(\pi u)}. \quad (5.13)$$

This gives

$$\langle j^\phi \rangle|_{m=0} = \frac{e \sin \alpha_p}{2\pi^3 w^2} \int_0^\infty du \frac{u \tanh u}{\cosh(2\alpha u) - \cos \alpha_p}. \quad (5.14)$$

The right-hand side of (5.14) describes the leading behavior of the current density for a massive field near the cone apex: $\langle j^\phi \rangle \approx \langle j^\phi \rangle|_{m=0}$ for $mw \ll 1$. For massive fields and at large distances, assuming $mw \gg 1$, the current density is suppressed by the factor $e^{-2mw \sin(\pi\alpha)}$ for $1/2 \leq \alpha < 1$ and by the factor e^{-2mw} in the case $\alpha \leq 1/2$.

6 Hadamard function and the current density on the Beltrami pseudosphere

In this section we specify the general results described above for the curved geometry corresponding to the Beltrami pseudosphere.

6.1 Mode functions

For the Beltrami pseudosphere the line element has the form (2.17). Introducing a new coordinate r in accordance with

$$r = ae^{-w/a}, \quad 0 \leq r < \infty, \quad (6.1)$$

the corresponding expression takes the form

$$ds^2 = dt^2 - \frac{a^2}{r^2} (dr^2 + L^2 d\phi^2). \quad (6.2)$$

For the part of the manifold that can be embedded in a 3-dimensional Euclidean space one has $r \geq L$. Note that the geometry (6.2) is conformally related to the 2D Rindler spacetime described by the line element $ds_{\text{R}}^2 = r^2 d\tau^2 - dr^2 - dy^2$ with dimensionless time coordinate $\tau = t/a$ and compact coordinate $y = L\phi$:

$$ds^2 = \frac{a^2}{r^2} ds_{\text{R}}^2. \quad (6.3)$$

The current densities in Rindler spacetime with a toroidally compact subspace in general number of spatial dimensions have been recently investigated in [64].

For the Beltrami pseudosphere the equation (3.5) is rewritten as

$$z''_{\sigma}(r) + \left(\frac{2\xi + a^2\lambda^2}{r^2} - \frac{k_n^2}{L^2} \right) z_{\sigma}(r) = 0, \quad (6.4)$$

with the general solution

$$z_{\sigma}(r) = \sqrt{y} [c_1 I_{i\nu}(y) + c_2 K_{i\nu}(y)], \quad y = |k_n|r/L. \quad (6.5)$$

Here $I_{\mu}(y)$ is the modified Bessel function and $\nu = \sqrt{a^2\lambda^2 + 2\xi - 1/4}$. As quantum numbers specifying the mode functions we can take the set $\sigma = (\nu, n)$. For the energy of a given mode we get

$$\omega = \frac{1}{a} \sqrt{\nu^2 + \nu_m^2}, \quad (6.6)$$

where

$$\nu_m^2 = m^2 a^2 + 1/4 - 2\xi. \quad (6.7)$$

For a conformally coupled field one has $\nu_m = ma$.

From the normalizability condition for the mode function it follows that $c_1 = 0$. The normalization condition (3.7), written in terms of the coordinate r , takes the form

$$2\pi L a^2 |c_2|^2 \int_0^{\infty} \frac{dy}{y} K_{i\nu}(y) K_{i\nu'}(y) = \frac{\delta(\nu - \nu')}{2\omega}. \quad (6.8)$$

By taking into account that $K_{-i\nu}(y) = K_{i\nu}(y)$, for the quantum number ν one has $0 < \nu < \infty$. Note that for the values of the curvature coupling parameter in the range $2\xi > m^2 a^2 + 1/4$ the energy becomes imaginary for the modes with $\nu^2 < 2\xi - m^2 a^2 - 1/4$. This leads to the instability of the vacuum state. In the discussion below we will assume that $2\xi \leq m^2 a^2 + 1/4$. In particular, this condition is satisfied

by the most important special cases of minimally ($\xi = 0$) and conformally ($\xi = 1/8$) coupled fields. By using the integration formula [65]

$$\int_0^\infty \frac{dy}{y} K_{i\nu}(y) K_{i\nu'}(y) = \frac{\pi^2 \delta(\nu - \nu')}{2\nu \sinh(\nu\pi)}, \quad (6.9)$$

for the normalization coefficient we find

$$c_2 = \sqrt{\frac{\nu \sinh(\nu\pi)}{2\pi^3 L a^2 \omega}}. \quad (6.10)$$

Hence, the normalized mode functions (3.4) take the form

$$\varphi_\sigma^{(\pm)}(x) = \sqrt{\frac{\nu \sinh(\nu\pi) y}{2\pi^3 L a^2 \omega}} K_{i\nu}(y) e^{ik_n \phi \mp i\omega t}, \quad y = |k_n| r/L, \quad (6.11)$$

with $k_w = \nu$ and ω given by (6.6). Note that the corresponding function

$$z_\sigma(w) = z_{k_w}(w, |k_n|) = c_2 \sqrt{y} K_{i\nu}(y) \quad (6.12)$$

is real.

6.2 Hadamard function

Having the mode functions, for the Hadamard function we get

$$\begin{aligned} G(x, x') &= \frac{\sqrt{rr'}}{\pi^3 L a^2} \sum_{n=-\infty}^{+\infty} e^{ik_n \Delta \phi} \int_0^\infty d\nu \frac{\nu}{\omega} \sinh(\nu\pi) \\ &\quad \times K_{i\nu}(|k_n| r/L) K_{i\nu}(|k_n| r'/L) \cos(\omega \Delta t), \end{aligned} \quad (6.13)$$

with ω from (6.6). For the corresponding function in the geometry (6.2) with uncompactified coordinate ϕ , $-\infty < \phi < +\infty$, one has

$$G_0(x, x') = \frac{2\sqrt{rr'}}{\pi^3 L a^2} \int_0^\infty du \cos(u \Delta \phi) \int_0^\infty d\nu \frac{\nu}{\omega} \sinh(\nu\pi) K_{i\nu}(ur/L) K_{i\nu}(ur'/L) \cos(\omega \Delta t). \quad (6.14)$$

The integral over u is evaluated by using the formula [63]

$$\int_0^\infty du \cos(u \Delta \phi) K_{i\nu}(ur/L) K_{i\nu}(ur'/L) = \frac{L\pi^2}{4\sqrt{rr'} \cosh(\nu\pi)} P_{i\nu-1/2} \left(\frac{r^2 + r'^2 + (L\Delta\phi)^2}{2rr'} \right), \quad (6.15)$$

where $P_{i\nu-1/2}(x)$ is the Legendre function. This gives

$$G_0(x, x') = \frac{a^{-2}}{2\pi} \int_0^\infty d\nu \frac{\nu}{\omega} \tanh(\nu\pi) \cos(\omega \Delta t) P_{i\nu-1/2} \left(\frac{r^2 + r'^2 + (L\Delta\phi)^2}{2rr'} \right). \quad (6.16)$$

The Hadamard function is decomposed as (3.16). For the function appearing in the topological part one has

$$z_{k_w}(w, iu) z_{k_w}^*(w', iu) - z_{k_w}(w, -iu) z_{k_w}^*(w', -iu) = i \frac{\sqrt{rr'}}{2\pi L a^2 \omega} \text{Im}[J_{i\nu}(ur/L) J_{i\nu}(ur'/L)], \quad (6.17)$$

where we have used the relation

$$\text{Im}[K_{i\nu}(iy) K_{i\nu}(iy')] = \frac{\pi^2}{2} \frac{\text{Im}[J_{i\nu}(y) J_{i\nu}(y')]}{\sinh(\nu\pi)}. \quad (6.18)$$

Hence, the Hadamard function is decomposed as

$$G(x, x') = G_0(x, x') - \frac{\sqrt{rr'}}{\pi La^2} \int_0^\infty d\nu \frac{\nu}{\omega} \cos(\omega \Delta t) \times \int_0^\infty du \operatorname{Im}[J_{i\nu}(ur/L)J_{i\nu}(ur'/L)] \sum_{s=\pm 1} \frac{e^{-su\Delta\phi}}{e^{2\pi u + is\alpha_p} - 1}. \quad (6.19)$$

We can further transform this formula by using the expansion $1/(e^y - 1) = \sum_{l=1}^\infty e^{-ly}$. With this expansion, the integral over u is expressed in terms of the Legendre function $Q_\mu(x)$:

$$G(x, x') = G_0(x, x') - \frac{a^{-2}}{\pi^2} \sum_{l=-\infty}^{+\infty} e^{-l\alpha_p} \int_0^\infty d\nu \frac{\nu}{\omega} \cos(\omega \Delta t) \times \operatorname{Im} \left[Q_{i\nu-1/2} \left(\frac{r^2 + r'^2 + L^2 (2\pi l + s\Delta\phi)^2}{2rr'} \right) \right], \quad (6.20)$$

where the prime on the summation sign means that the term $l = 0$ should be omitted. Now, by using the relation between the Legendre functions [62], we can see that (note that the function $P_{i\nu-1/2}(z)$ is a real function for real ν and z)

$$\operatorname{Im}[Q_{i\nu-1/2}(z)] = -\frac{\pi}{2} \tanh(\pi\nu) P_{i\nu-1/2}(z). \quad (6.21)$$

By taking into account the expression (6.14) for the function $G_0(x, x')$, the final expression is written in the form

$$G(x, x') = \frac{a^{-2}}{2\pi} \sum_{l=-\infty}^\infty e^{-il\alpha_p} \int_0^\infty d\nu \frac{\nu}{\omega} \tanh(\pi\nu) \cos(\omega \Delta t) P_{i\nu-1/2} \left(\frac{r^2 + r'^2 + L^2 (\Delta\phi + 2\pi l)^2}{2rr'} \right). \quad (6.22)$$

where the $l = 0$ term corresponds to the function $G_0(x, x')$.

The formula (6.22) could also be obtained in another way, by using the integral representation [66]

$$K_{i\nu}(br)K_{i\nu}(br') = \frac{1}{2} \int_0^\infty \frac{dy}{y} \exp\left(-\frac{y}{2} - b^2 \frac{r^2 + r'^2}{2y}\right) K_{i\nu}(b^2 rr'/y)$$

for the product of the Macdonald functions in (6.13). This gives

$$G(x, x') = \frac{\sqrt{rr'}}{2\pi^3 La^2} \sum_{n=-\infty}^{+\infty} e^{ik_n \Delta\phi} \int_0^\infty d\nu \frac{\nu}{\omega} \sinh(\nu\pi) \cos(\omega \Delta t) \times \int_0^\infty \frac{du}{u} \exp\left(-\frac{k_n^2}{2uL^2} - u \frac{r^2 + r'^2}{2}\right) K_{i\nu}(rr'u), \quad (6.23)$$

where we have introduced a new integration variable $u = k_n^2/(L^2 y)$. As the next step we apply the Poisson resummation formula to the series over n . The following relation is obtained:

$$\sum_{n=-\infty}^{+\infty} \exp\left(ik_n \Delta\phi - \frac{k_n^2}{2uL^2}\right) = L\sqrt{2\pi u} \sum_{l=-\infty}^\infty \exp\left[-il\alpha_p - \frac{u}{2} L^2 (\Delta\phi + 2\pi l)^2\right]. \quad (6.24)$$

Substituting this in (6.23), the integral over u is evaluated with the help of the formula

$$\int_0^\infty \frac{du}{\sqrt{u}} e^{-pu} K_{i\nu}(cu) = \frac{\pi^{3/2} P_{i\nu-1/2}(p/c)}{\sqrt{2c} \cosh(\pi\nu)},$$

and we obtain the representation (6.22).

Another representation for the Hadamard function is obtained from (6.23) by taking into account the relation (6.24):

$$G(x, x') = \frac{\sqrt{rr'}/2}{\pi^{5/2}a^2} \sum_{l=-\infty}^{\infty} e^{-il\alpha_p} \int_0^{\infty} \frac{du}{\sqrt{u}} \exp \left[-\frac{u}{2} \left(r^2 + r'^2 + L^2 (\Delta\phi + 2\pi l)^2 \right) \right] \\ \times \int_0^{\infty} d\nu \frac{\nu}{\omega} \sinh(\nu\pi) \cos(\omega\Delta t) K_{i\nu}(rr'u), \quad (6.25)$$

By using the formula

$$\sinh(\pi\nu) K_{i\nu}(z) = \frac{\pi i}{2} [I_{i\nu}(z) - I_{-i\nu}(z)], \quad (6.26)$$

for the Macdonald function, this gives

$$G(x, x') = \frac{i\sqrt{rr'}}{(2\pi)^{3/2}a^2} \sum_{l=-\infty}^{\infty} e^{-il\alpha_p} \int_0^{\infty} \frac{du}{\sqrt{u}} \exp \left[-\frac{u}{2} \left(r^2 + r'^2 + L^2 (\Delta\phi + 2\pi l)^2 \right) \right] \\ \times \int_0^{\infty} d\nu \frac{\nu}{\omega} \sinh(\nu\pi) \cos(\omega\Delta t) [I_{i\nu}(rr'u) - I_{-i\nu}(rr'u)], \quad (6.27)$$

We rotate the integration contour over ν by the angle $\pi/2$ for the term with $I_{-i\nu}(xx'u)$ and by the angle $-\pi/2$ for the term with $I_{i\nu}(xx'u)$. Assuming that $\nu_m^2 \geq 0$, for the integral we get

$$\int_0^{\infty} d\nu \frac{\nu}{\omega} \cos(\omega\Delta t) [I_{i\nu}(rr'u) - I_{-i\nu}(rr'u)] = \frac{2}{i} a \int_{\nu_m}^{\infty} d\nu \frac{\nu \cosh(\sqrt{\nu^2 - \nu_m^2} \Delta t/a)}{\sqrt{\nu^2 - \nu_m^2}} I_{\nu}(rr'u). \quad (6.28)$$

By using the integration formula [63]

$$\int_0^{\infty} \frac{du}{\sqrt{u}} e^{-bu/2} I_{\nu}(rr'u) = \sqrt{\frac{2}{\pi rr'}} Q_{\nu-1/2} \left(\frac{b}{2rr'} \right), \quad (6.29)$$

for the Hadamard function we find the representation

$$G(x, x') = \frac{1}{\pi^2 a} \sum_{l=-\infty}^{\infty} e^{il\alpha_p} \int_{\nu_m}^{\infty} d\nu \frac{\nu \cosh(\sqrt{\nu^2 - \nu_m^2} \Delta t/a)}{\sqrt{\nu^2 - \nu_m^2}} Q_{\nu-1/2} \left(\frac{r^2 + r'^2 + L^2 (\Delta\phi - 2\pi l)^2}{2rr'} \right). \quad (6.30)$$

Note that the Legendre function in this formula is expressed in terms of the hypergeometric function as

$$Q_{\nu-1/2}(z) = \frac{\sqrt{\pi} \Gamma(\nu + 1/2)}{(2z)^{\nu+1/2} \Gamma(\nu + 2)} F \left(\frac{\nu + 3/2}{2}, \frac{\nu + 1/2}{2}; \nu + 1, \frac{1}{z^2} \right). \quad (6.31)$$

As it is seen from (2.17), the geometry of cylindrical tube with constant radius is obtained from the case of the Beltrami pseudosphere in the limit $a \rightarrow 0$ for fixed w . From (6.1) it follows that the coordinate r is large in that limit and for the argument of the Legendre function in (6.30) one has

$$\frac{r^2 + r'^2 + L^2 (\Delta\phi - 2\pi l)^2}{2rr'} \approx 1 + \frac{(\Delta x_l)^2}{2a^2}, \quad \Delta x_l = \sqrt{(\Delta w)^2 + L^2 (\Delta\phi - 2\pi l)^2}. \quad (6.32)$$

By taking into account that in the limit under consideration ν_m is large, we use the asymptotic formula for the Legendre function [67]

$$Q_{\nu-1/2}(\cosh u) \approx \left(\frac{u}{\sinh u} \right)^{1/2} K_0(\nu u), \quad \nu \gg 1. \quad (6.33)$$

For the function in (6.30) one has $u \approx a\Delta x_l$. Substituting (6.33) in (6.30) and redefining the integration variable as $a\nu \rightarrow \nu$, in the leading order we get

$$G(x, x') \approx \frac{1}{\pi^2} \sum_{l=-\infty}^{\infty} e^{il\alpha_p} \int_m^{\infty} d\nu \frac{\nu \cosh(\Delta t \sqrt{\nu^2 - m^2})}{\sqrt{\nu^2 - m^2}} K_0(\nu \Delta x_l). \quad (6.34)$$

The integral is evaluated by using the formula from [63] with the result

$$G(x, x') \approx \frac{1}{2\pi} \sum_{l=-\infty}^{\infty} \frac{e^{il\alpha_p} e^{-m\sqrt{(\Delta x_l)^2 - (\Delta t)^2}}}{\sqrt{(\Delta x_l)^2 - (\Delta t)^2}}. \quad (6.35)$$

The expression on the right-hand side coincides with the Hadamard function for a cylindrical tube of constant radius (see, for example, [15]).

6.3 Current density

Similar to the case of conical geometry the function $z_{k_w}(w, u)$ is real for real u (see (6.12)) and $C_{k_w}(u) = 0$. Hence, the current density along the axial direction vanishes, $\langle j^1 \rangle = 0$. The VEV of the current density in the compact dimension is obtained from the general formula (4.6). By using (6.12) we get

$$\langle j^\phi \rangle = -\frac{er^2}{\pi L^2 a^2} \sin \alpha_p \int_0^{\infty} d\nu \frac{\nu}{\sqrt{\nu^2 + \nu_m^2}} \int_0^{\infty} du \frac{u \operatorname{Im}[J_{i\nu}^2(ur/L)]}{\cosh(2\pi u) - \cos \alpha_p}. \quad (6.36)$$

As seen, the current density depends on r and L in the form of the ratio

$$\frac{L}{r} = \frac{L}{a} e^{w/a}. \quad (6.37)$$

For a fixed w , the proper length of the compact dimension is given by $2\pi L e^{w/a}$. The current density is an odd periodic function of the parameter α_p with the period 2π . This corresponds to periodicity with respect to the magnetic flux with the period of flux quantum. An alternative representation is obtained by using the formula (6.22) for the Hadamard function:

$$\langle j^\phi \rangle = -\frac{2eL}{ra^2} \sum_{l=1}^{\infty} l \sin(l\alpha_p) \int_0^{\infty} d\nu \frac{\nu \tanh(\pi\nu)}{\sqrt{\nu^2 + \nu_m^2}} P'_{i\nu-1/2} \left(1 + 2(\pi l L/r)^2 \right), \quad (6.38)$$

where the prime means the derivative with respect to the argument of the function.

Another representation for the current density is obtained from (6.30) by using (4.2):

$$\langle j^\phi \rangle = -\frac{4eL}{\pi r a^2} \sum_{l=1}^{\infty} l \sin(l\alpha_p) \int_{\nu_m}^{\infty} d\nu \nu \frac{Q'_{\nu-1/2} \left(1 + 2(\pi l L/r)^2 \right)}{\sqrt{\nu^2 - \nu_m^2}}. \quad (6.39)$$

In the limit $a \rightarrow \infty$, with fixed value of w , the parameter ν and the coordinate r are large and we use the asymptotic (6.33) for the Legendre function. It can be seen that in the leading order from (6.39) the result (5.3) is obtained for the current density in a cylindrical tube with constant radius.

Let us consider the behavior of the current density in the asymptotic regions of the ratio r/L . For $r/L \ll 1$ the argument of the Legendre function in (6.39) is large and we use the formula [67]

$$Q_{\nu-1/2}(x) \approx \frac{\sqrt{\pi} \Gamma(\nu + 1/2)}{\Gamma(\nu + 1) (2x)^{\nu+1/2}}, \quad (6.40)$$

for $x \gg 1$. In the leading order this gives

$$\langle j^\phi \rangle \approx \frac{e(r/L)^2}{\pi^{7/2}a^2} \sum_{l=1}^{\infty} \frac{\sin(l\alpha_p)}{l^2} \int_{\nu_m}^{\infty} d\nu \frac{\Gamma(\nu + 3/2) e^{-2\nu \ln(2\pi l)}}{\Gamma(\nu) \sqrt{\nu^2 - \nu_m^2}}, \quad (6.41)$$

and the current density tends to zero like $(r/L)^2$. In the opposite limit $r/L \gg 1$ the dominant contribution to the integral in (6.39) comes from large ν and we employ the asymptotic (6.33). The integral is evaluated by using the formula from [63] and the leading order term is expressed as

$$\langle j^\phi \rangle \approx \frac{er^2}{4\pi^3 L^2 a^2} \sum_{l=1}^{\infty} \frac{\sin(l\alpha_p)}{l^2}, \quad r \gg L. \quad (6.42)$$

For a given r the radius of the tube is given by aL/r and the limit under consideration corresponds to the region where the radius of the tube is much smaller than the curvature radius a .

For a conformally coupled massless field we have $\nu_m = 0$ and the expression for the current density is transformed to

$$\langle j^\phi \rangle = -\frac{4eL}{\pi r a^2} \sum_{l=1}^{\infty} l \sin(l\alpha_p) \int_0^{\infty} d\nu Q'_{\nu-1/2} \left(1 + 2(\pi l L/r)^2 \right). \quad (6.43)$$

As it has been mentioned above, the geometry at hand is conformally related to the 2D Rindler spacetime with a compact dimension (see (6.3)). For a conformally coupled massless field we expect the relation

$$\langle j^\phi \rangle = \frac{r^2}{a^2} \langle j^\phi \rangle_{\text{R}}, \quad (6.44)$$

where $\langle j^\phi \rangle_{\text{R}}$ is the current density in the Rindler spacetime. The expression for the latter is obtained from the general formula in [64] taking $D = 2$ for spatial dimension and making the replacement $L \rightarrow 2\pi L$:

$$\langle j^\phi \rangle_{\text{R}} = \frac{eL}{4r^3} \sum_{l=1}^{\infty} l \sin(l\alpha_p) \left\{ \frac{1}{(\pi l L/r)^3} - \int_0^{\infty} dx \frac{[\cosh^2 x + (\pi l L/r)^2]^{-\frac{3}{2}}}{x^2 + \pi^2/4} \right\}. \quad (6.45)$$

We have checked numerically that the following relation is valid:

$$\int_0^{\infty} d\nu Q_{\nu-1/2} (1 + 2u^2) = \frac{\pi}{4} \left[\frac{1}{u} - \int_0^{\infty} d\nu \frac{(\cosh^2 \nu + u^2)^{-\frac{1}{2}}}{\nu^2 + \pi^2/4} \right]. \quad (6.46)$$

This relation shows that the connection (6.44) indeed takes place between the current densities on the Beltrami pseudosphere and in 2D Rindler spacetime with compact dimension.

The left panel of Fig. 3 presents the dependence of the current density on the mass of the field for $L/r = 0.5$ and $\alpha_p = 2\pi/5$. The right panel displays the current density versus $\alpha_p/2\pi$ for the same value of L/r and for $ma = 0.5$. On both panels the numbers near the curves are the corresponding values of the curvature coupling parameter.

In Fig. 4 we have plotted the dependence of the current density on the ratio L/r for minimally and conformally coupled massless fields. The graphs are plotted for $\alpha_p = \pi/2$. As was expected, the current density tends to zero in the limit $L/r \rightarrow \infty$.

It is of interest to compare the vacuum current densities for different geometries of the 2D tube. The solid curves in Fig. 5 present the ratio of the current densities on the Beltrami pseudosphere and on the tube with a constant radius, $\langle j^\phi \rangle / \langle j^\phi \rangle_c$, as a function of the proper radius $L_{(p)}$ of the tube in units of the curvature radius a . For the Beltrami pseudosphere $L_{(p)} = aL/r$ and for the tube with constant radius $L_{(p)} = L$. The current density for the tube with a constant radius is given by (5.3) and the ratio $\langle j^\phi \rangle / \langle j^\phi \rangle_c$ is evaluated for the same values of the proper radii for the Beltrami pseudosphere and

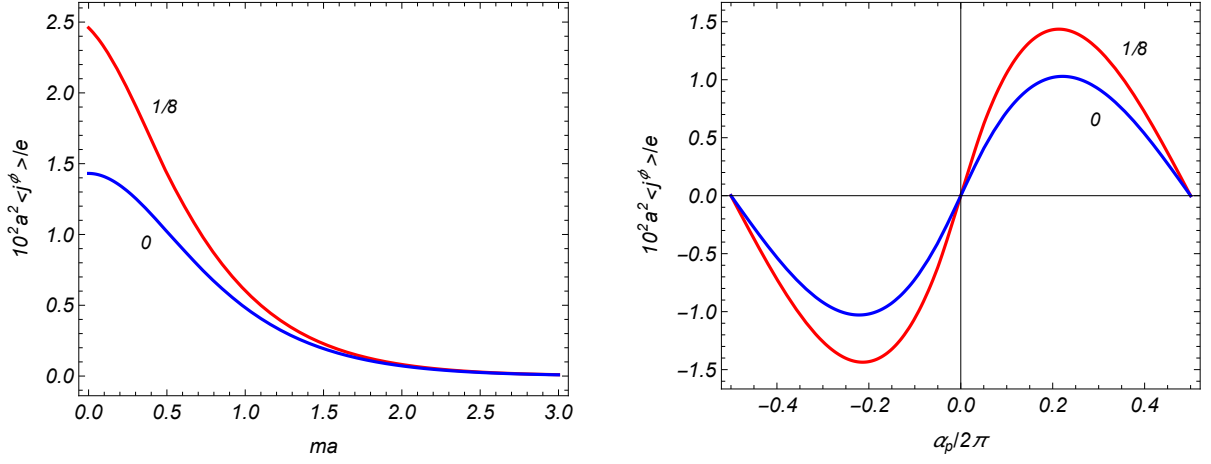


Figure 3: The current density as a function of the mass (left panel) and of the phase in the quasiperiodicity condition (right panel) for $L/r = 0.5$. For the left panel we have taken $\alpha_p = 2\pi/5$ and for the right panel $ma = 0.5$.

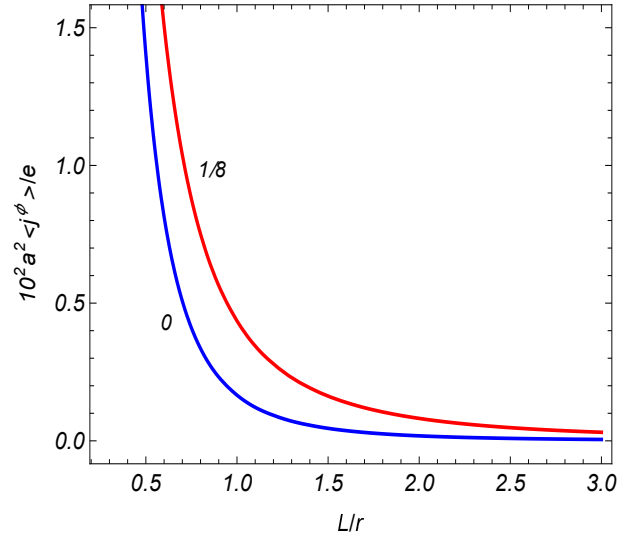


Figure 4: The current density versus L/r for conformally ($\xi = 1/8$) and minimally ($\xi = 0$) coupled massless fields and for fixed $\alpha_p = \pi/2$.

constant radius tube. The dashed lines in Fig. 5 present the same ratio for the AdS tube instead of the Beltrami pseudosphere. The proper radius for the AdS tube one has $L_{(p)} = aL/z$ and the corresponding current density is given by (A.7). The graphs in Fig. 5 are plotted for $ma = 0.5$, $\alpha_p = \pi/2$, and the numbers near the curves are the corresponding values of the curvature coupling parameter ξ . As seen from the graphs, for large values of the proper radius of the tube one has $\langle j^\phi \rangle / \langle j^\phi \rangle_c \gg 1$ for both the Beltrami pseudosphere and AdS tube. This is related to the fact that in that range the decay of the current densities for the Beltrami pseudosphere and AdS tube, as functions of the proper radius, follows a power-law, whereas for a constant radius tube the decay is exponential for a massive field.

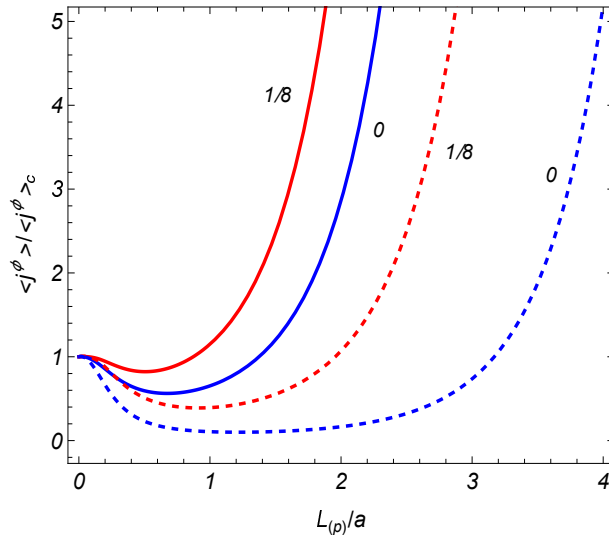


Figure 5: The ratio of the current densities on the Beltrami pseudosphere and on the tube with constant radius (full curves) versus the proper radius of the tube in units of the curvature radius a . The dashed curves present the same ratio for the AdS tube and the tube of constant radius. The graphs are plotted for conformally and minimally coupled fields and for $ma = 0.5$, $\alpha_p = \pi/2$.

7 Conclusion

We have investigated combined effects of spatial curvature and topology on the local properties of the ground state for a quantum scalar field in (2+1)-dimensional spacetime. The corresponding line element has the form (2.4) and it describes rotationally symmetric 2D curved tube with general dependence of the radius on the axial coordinate. As special cases, a cylindrical tube with a constant radius, conical tube and tubes with constant positive and negative curvature are considered. The local properties of the vacuum state are encoded in two-point functions. As such, the Hadamard function is taken. It is evaluated by using the mode-sum formula (3.9) with scalar field modes given by (3.4) and obeying the quasiperiodicity condition (3.3) with a general phase α_p . The dependence of the mode functions on the axial coordinate is expressed in terms of the function $z_\sigma(w)$ being the solution of the equation (3.5) and normalized by the condition (3.7).

In order to extract the effects induced by the compactification, we have separated from the Hadamard function the part that corresponds to the same local geometry with decompactified ϕ -coordinate. The separation is done by using the Abel-Plana-type summation formula and the decomposed representation of the Hadamard function is given by (3.16). The VEVs of local physical observables, bilinear in the field operator, are obtained from the Hadamard function and its derivatives in the coincidence limit of the spacetime arguments. That limit is divergent and a renormalization procedure is required to extract finite physical values of the VEVs. The advantage of the presentation (3.16) is that the difference

$G(x, x') - G_0(x, x')$ is finite in the coincidence limit $x' \rightarrow x$ and the last term can be directly used for the evaluation of renormalized topological contributions in the VEVs.

As an important physical characteristic of the vacuum state we have considered the expectation value of the current density. The general expressions for the currents in the axial and angular directions are given by (4.3) and (4.6). In the special cases of constant radius and conical tubes the axial current vanishes and the general formulas for the current along compact dimension are reduced to the results previously investigated in the literature. For a conical tube, a new representation (5.9) is provided. As another application of general formulas, in Section 6 the Hadamard function and the current density on the Beltrami pseudosphere are studied. The corresponding mode functions are given by (6.12) and the Hadamard function is expressed as (6.13). An alternative expression is provided by formula (6.30). The component of the vacuum current along the axial direction vanishes and for the VEV of the component along the compact dimension we have provided several representations (see (6.36), (6.38) and (6.39)). The spacetime geometry for the Beltrami pseudosphere is conformally related to the one for 2D Rindler spacetime (see (6.3)) and we have shown that for a conformally coupled massless field the standard relation between the corresponding VEVs in conformally connected problems take place. For a massive field with general curvature coupling the dimensionless combination $a^2 \langle j^\phi \rangle$ is a function of the ratio L/r which gives the proper radius of compact dimension measured in units of the curvature radius a . For the radius of the tube much smaller than the curvature radius, $L/r \ll 1$, the effect of the spatial curvature on the current density is weak and, in the leading order, the VEV coincides with the corresponding current density for a tube with a constant radius equal to the proper radius aL/r (see (6.42)). In the opposite limit of large proper radius, $L/r \gg 1$, the effect of curvature is essential and the asymptotic is described by (6.41). In this limit, the decay of the current density as a function of the proper radius follows a power-law, like $(r/L)^2$. This behavior is in clear contrast to the one for a constant radius tube when the current density for a massive field is suppressed exponentially.

Acknowledgments

The work was supported by the grant No. 21AG-1C047 of the Higher Education and Science Committee of the Ministry of Education, Science, Culture and Sport RA and by the ANSEF grant 23AN:PS-hepth-2889.

A Vacuum currents in locally dS and AdS tubes

The vacuum currents for a scalar field in locally dS and AdS spacetimes with toroidal subspaces for general number of spatial dimension have been considered in Refs. [54] and [55], respectively (for a review and further discussions see also [7]). Here we specify the corresponding results for the case of 2D space with a single compact dimension (dS and AdS tubes).

For dS tubes the line element reads

$$ds_{\text{dS}}^2 = dt^2 - e^{-2t/a} (dw^2 + L^2 d\phi^2). \quad (\text{A.1})$$

For the Ricci scalar one has $R = 6/a^2$ and the nonzero components of the Ricci tensor are given by (no summation over i) $R_i^i = 2/a^2$, $i = 0, 1, 2$. From the general result of [54] for the physical component of the current density along the compact dimension we get

$$\langle j^\phi \rangle_{\text{dS}} = -\frac{2eL}{a^2\eta} \sum_{l=1}^{\infty} l \sin(l\alpha_p) \partial_u F_{\nu_-}^{(\text{dS})}(u), \quad u = 2 \left(\pi l \frac{L}{\eta} \right)^2 - 1, \quad (\text{A.2})$$

where

$$\eta = ae^{t/a}, \quad \nu_{\pm} = \sqrt{1 - 6\xi \pm m^2 a^2}. \quad (\text{A.3})$$

In (A.2) we have defined the function

$$\begin{aligned} F_\nu^{(\text{dS})}(u) &= \frac{\sinh \nu x}{\sin(\pi\nu) \sinh x}, \quad x = \text{arccosh } u, \text{ for } u \geq 1, \\ F_\nu^{(\text{dS})}(u) &= \frac{\sin \nu x}{\sin(\pi\nu) \sin x}, \quad x = \arccos u, \text{ for } u \leq 1. \end{aligned} \quad (\text{A.4})$$

In deriving (A.2) it was assumed that the field is prepared in the Bunch-Davies vacuum state. The parameter ν can be either positive or purely imaginary. Note that $\tau = -\eta$, $-\infty < \tau < 0$ is the conformal time in terms of which the line element is written in conformally flat form $ds_{\text{dS}}^2 = (a/\tau)^2 (d\tau^2 - dw^2 - L^2 d\phi^2)$. In the case of a conformally coupled massless field one has $\nu_- = 1/2$ and for the function (A.4) we find $F_\nu^{(\text{dS})}(u) = 2^{3/2}/\sqrt{u+1}$. For the current density this gives

$$\langle j^\phi \rangle_{\text{dS}} = \frac{e\eta^2}{4\pi^3 L^2 a^2} \sum_{l=1}^{\infty} \frac{\sin(l\alpha_p)}{l^2}. \quad (\text{A.5})$$

As expected, in this special case we have the conformal relation $\langle j^\phi \rangle_{\text{dS}} = (\eta/a)^2 \langle j^\phi \rangle$, where $\langle j^\phi \rangle$ is the current density for a massless field on a cylindrical tube with constant radius (see (5.3) for $m = 0$).

In the case of AdS tubes the line element has the form

$$ds_{\text{AdS}}^2 = e^{2w/a} (dt^2 - L^2 d\phi^2) - dw^2, \quad (\text{A.6})$$

with the curvature scalar and Ricci tensor $R = -6/a^2$ and $R_i^i = -2/a^2$ (no summation over i). The expression for the vacuum current density is obtained from the general formula in Ref. [55]:

$$\langle j^\phi \rangle_{\text{AdS}} = -\frac{2eL}{a^2 z} \sum_{l=1}^{\infty} l \sin(l\alpha_p) \partial_u F_{\nu_+}^{(\text{AdS})}(u), \quad u = 2 \left(\pi l \frac{L}{z} \right)^2 + 1, \quad (\text{A.7})$$

with $z = ae^{w/a}$, $0 < z < \infty$, and

$$F_\nu^{(\text{AdS})}(u) = \frac{e^{-\nu x}}{\sinh x}, \quad x = \text{arccosh } u. \quad (\text{A.8})$$

With the new axial coordinate z , the line element is presented in a conformally flat form $ds_{\text{AdS}}^2 = (a/z)^2 (d\tau^2 - dz^2 - L^2 d\phi^2)$. The circles $z = 0$ and $z = \infty$ correspond to the AdS boundary and horizon.

For a conformally coupled massless field $\nu_+ = 1/2$ and

$$F_\nu^{(\text{AdS})}(u) = \frac{1}{\sqrt{2}} \left(\frac{1}{\sqrt{u-1}} - \frac{1}{\sqrt{u+1}} \right). \quad (\text{A.9})$$

Putting this in (A.7) one gets $\langle j^\phi \rangle_{\text{AdS}} = (z/a)^2 \langle j^\phi \rangle_{(1)}$, where

$$\langle j^\phi \rangle_{(1)} = \frac{e}{4\pi^3 L^2} \sum_{l=1}^{\infty} \frac{\sin(l\alpha_p)}{l^2} \left\{ 1 - \left[1 + \left(\frac{z}{\pi l L} \right)^2 \right]^{-3/2} \right\}. \quad (\text{A.10})$$

We have a conformal relations between the current densities on AdS tube and on a cylindrical tube with constant radius having a circular edge at $z = 0$. On the latter the field obeys the Dirichlet boundary condition. The presence of the edge in the Minkowski counterpart is related to the boundary condition for the field on the AdS boundary. The edge $z = 0$ in the Minkowskian problem is the conformal image of the AdS boundary. Hence, formula (A.10) provides the expression of the current density for a massless scalar field with the boundary condition $\varphi(x) = 0$ on the edge $z = 0$ of a cylindrical surface with constant radius. The effects of edges of AdS tubes on the vacuum current densities for scalar and fermionic fields are discussed in [68, 69, 70, 71].

References

- [1] N.D. Birrell, P.C.W. Davies, *Quantum Fields in Curved Space* (Cambridge University Press, Cambridge, England, 1982).
- [2] A.A. Grib, S.G. Mamayev, V.M. Mostepanenko, *Vacuum Quantum Effects in Strong Fields* (Friedmann Laboratory Publishing, St. Petersburg, 1994).
- [3] L.E. Parker, D.J. Toms, *Quantum Field Theory in Curved Spacetime* (Cambridge University Press, Cambridge, England, 2009).
- [4] G.V. Dunne, *Topological Aspects of Low Dimensional Systems* (Springer, Berlin, 1999).
- [5] Y. Imry, *Introduction to Mesoscopic Physics* (Oxford University Press, New York, USA, 2008).
- [6] V.M. Fomin (Ed.), *Physics of Quantum Rings* (Springer International Publishing, Cham, Switzerland, 2018).
- [7] A.A. Saharian, Vacuum currents for a scalar field in models with compact dimensions, *Symmetry* **16**, 92 (2024).
- [8] A.C. Bleszynski-Jayich, W.E. Shanks, B. Peaudecerf, E. Ginossar, F. von Oppen, L. Glazman, J.G.E. Harris, Persistent currents in normal metal rings, *Science* **326**, 272 (2009).
- [9] H. Bluhm, N.C. Koshnick, J.A. Bert, M.E. Huber, K.A. Moler, Persistent currents in normal metal rings, *Phys. Rev. Lett.* **102**, 136802 (2009).
- [10] S. Deser, R. Jackiw, S. Templeton, Topologically massive gauge theories, *Ann. Phys. (N.Y.)* **140**, 372 (1982).
- [11] V.P. Gusynin, S.G. Sharapov, J.P. Carbotte, AC conductivity of graphene: From tight-binding model to 2+1-dimensional quantum electrodynamics, *Int. J. Mod. Phys. B* **21**, 4611 (2007).
- [12] A.H. Castro Neto, F. Guinea, N.M.R. Peres, K.S. Novoselov, A.K. Geim, The electronic properties of graphene, *Rev. Mod. Phys.* **81**, 109 (2009).
- [13] S. Bellucci, A.A. Saharian, N.A. Saharyan, Casimir effect for scalar current densities in topologically nontrivial spaces, *Eur. Phys. J. C* **75**, 378 (2015).
- [14] S. Bellucci, A.A. Saharian, V.M. Bardeghyan, Induced fermionic current in toroidally compactified spacetimes with applications to cylindrical and toroidal nanotubes, *Phys. Rev. D* **82**, 065011 (2010).
- [15] E.R. Bezerra de Mello, A.A. Saharian, Finite temperature current densities and Bose-Einstein condensation in topologically nontrivial spaces, *Phys. Rev. D* **87**, 045015 (2013).
- [16] S. Bellucci, E.R. Bezerra de Mello, A.A. Saharian, Finite temperature fermionic condensate and currents in topologically nontrivial spaces, *Phys. Rev. D* **89**, 085002 (2014).
- [17] L. Sriramkumar, Fluctuations in the current and energy densities around a magnetic-flux-carrying cosmic string, *Classical Quantum Gravity* **18**, 1015 (2001).
- [18] Yu.A. Sitenko and N.D. Vlasii, Induced vacuum current and magnetic field in the background of a cosmic string, *Classical Quantum Gravity* **26**, 195009 (2009).
- [19] E.R. Bezerra de Mello, Induced fermionic current densities by magnetic flux in higher dimensional cosmic string spacetime, *Classical Quantum Gravity* **27**, 095017 (2010).

- [20] Y.A. Sitenko, V.M. Gorkavenko, Non-Euclidean geometry, nontrivial topology and quantum vacuum effects, *Universe* **4**, 23 (2018).
- [21] E.R. Bezerra de Mello, V.B. Bezerra, A.A. Saharian, H.H. Harutyunyan, Vacuum currents induced by a magnetic flux around a cosmic string with finite core, *Phys. Rev. D* **91**, 064034 (2015).
- [22] E.R. Bezerra de Mello, A.A. Saharian, Fermionic current induced by magnetic flux in compactified cosmic string spacetime, *Eur. Phys. J. C* **73**, 2532 (2013).
- [23] E.A.F. Bragança, H.F. Santana Mota, E.R. Bezerra de Mello, Induced vacuum bosonic current by magnetic flux in a higher dimensional compactified cosmic string spacetime, *Int. J. Mod. Phys. D* **24**, 1550055 (2015).
- [24] S. Bellucci, A.A. Saharian, A.Kh. Grigoryan, Induced fermionic charge and current densities in two-dimensional rings, *Phys. Rev. D* **94**, 105007 (2016).
- [25] F. Guinea, M.I. Katsnelson, A.K. Geim, Energy gaps and a zero-field quantum Hall effect in graphene by strain engineering, *Nat. Phys.* **6**, 30 (2010).
- [26] N. Levy et al., Strain-induced pseudo-magnetic fields greater than 300 Tesla in graphene nanobubbles, *Science* **329**, 544 (2010).
- [27] M.A.H. Vozmediano, M.I. Katsnelson, F. Guinea, Gauge fields in graphene, *Phys. Rept.* **496**, 109 (2010).
- [28] J. González, F. Guinea, M.A.H. Vozmediano, The electronic spectrum of fullerenes from the Dirac equation, *Nucl. Phys. B* **406**, 771 (1993).
- [29] D.V. Kolesnikov, V.A. Osipov, The continuum gauge field-theory model for low-energy electronic states of icosahedral fullerenes, *Eur. Phys. J. B* **49**, 465 (2006).
- [30] A. Cortijo, M.A.H. Vozmediano, Effects of topological defects and local curvature on the electronic properties of planar graphene, *Nucl. Phys. B* **763**, 293 (2007).
- [31] M.A.H. Vozmediano, F. de Juan, A. Cortijo, Gauge fields and curvature in graphene, *J. Phys. Conf. Ser.* **129**, 012001 (2008).
- [32] D.-H. Lee, Surface states of topological insulators: The Dirac fermion in curved two-dimensional spaces, *Phys. Rev. Lett.* **103**, 196804 (2009).
- [33] J. González, J. Herrero, Graphene wormholes: A condensed matter illustration of Dirac fermions in curved space, *Nucl. Phys. B* **825**, 426 (2010).
- [34] A. Iorio, G. Lambiase, The Hawking-Unruh phenomenon on graphene, *Phys. Lett. B* **716**, 334 (2012).
- [35] M. Cvetič, G.W. Gibbons, Graphene and the Zermelo optical metric of the BTZ black hole, *Ann. Phys. (N.Y.)* **327**, 2617 (2012).
- [36] Y. Takane, K.-I. Imura, Unified description of Dirac electrons on a curved surface of topological insulators, *J. Phys. Soc. Japan* **82**, 074712 (2013).
- [37] A. Iorio, G. Lambiase, Quantum field theory in curved graphene spacetimes, Lobachevsky geometry, Weyl symmetry, Hawking effect, and all that, *Phys. Rev. D* **90**, 025006 (2014).
- [38] G.E. Volovik, M.A. Zubkov, Emergent Horava gravity in graphene, *Ann. Phys. (N.Y.)* **340**, 352 (2014).

- [39] M.A. Zubkov, G.E. Volovik, Emergent gravity in graphene, *J. Phys.: Conf. Ser.* **607**, 012020 (2015).
- [40] T. Stegmann, N. Szpak, Current flow paths in deformed graphene: from quantum transport to classical trajectories in curved space, *New J. Phys.* **18**, 053016 (2016).
- [41] S. Taioli, R. Gabbrielli, S. Simonucci, N.M. Pugno, A. Iorio, Lobachevsky crystallography made real through carbon pseudospheres, *J. Phys.: Condens. Matter* **28**, 13LT01 (2016).
- [42] L. Yu, A. Ruzsinszky, J.P. Perdew, Bending two-dimensional materials to control charge localization and fermi-level shift, *Nano Lett.* **16**, 2444 (2016).
- [43] P. Castro-Villarreal, R. Ruiz-Sánchez, Pseudomagnetic field in curved graphene, *Phys. Rev. B* **95**, 125432 (2017).
- [44] S. Capozziello, R. Pincak, E.N. Saridakis, Constructing superconductors by graphene Chern-Simons wormholes, *Ann. Phys. (N.Y.)* **390**, 303 (2018).
- [45] T. Rojjanason, P. Burikham, K. Pimsamarn, Charged fermion in $(1 + 2)$ -dimensional wormhole with axial magnetic field, *Eur. Phys. J. C* **79**, 660 (2019).
- [46] B.S. Kandemir, Hairy BTZ black hole and its analogue model in graphene, *Ann. Phys. (N.Y.)* **413**, 168064 (2020).
- [47] T. Morresi, D. Binosi, S. Simonucci, R. Piergallini, S. Roche, N.M. Pugno, T. Simone, Exploring event horizons and Hawking radiation through deformed graphene membranes, *2D Materials* **7**, 041006 (2020).
- [48] A. Sedrakyan, A. Sinner, K. Ziegler, Deformation of a graphene sheet: Interaction of fermions with phonons, *Phys. Rev. B* **103**, L201104 (2021).
- [49] A. Iorio, Carbon pseudospheres and the BTZ black hole, *PoS(CORFU2021)240*.
- [50] G. Alencar, V.B. Bezerra, C.R. Muniz, Casimir wormholes in 2+1 dimensions with applications to the graphene, *Eur. Phys. J. C* **81**, 924 (2021).
- [51] A. Gallerati, Negative-curvature spacetime solutions for graphene, *J. Phys.: Condens. Matter* **33**, 135501 (2021).
- [52] A. Gallerati, Graphene, Dirac equation and analogue gravity, *Phys. Scr.* **97**, 064005 (2022).
- [53] N. Wei, Y. Ding, J. Zhang, L. Li, M. Zeng, L. Fu, Curvature geometry in 2D materials, *Natl Sci Rev.* **10**, nwad145 (2023).
- [54] S. Bellucci, A.A. Saharian, H.A. Nersisyan, Scalar and fermionic vacuum currents in de Sitter spacetime with compact dimensions, *Phys. Rev. D* **88**, 024028 (2013).
- [55] E.R. Bezerra de Mello, A.A. Saharian, V. Vardanyan, Induced vacuum currents in anti-de Sitter space with toral dimensions, *Phys. Lett. B* **741**, 155 (2015).
- [56] A. Krishnan, E. Dujardin, M.M.J. Treacy, J. Hugdahl, S. Lynum, T.W. Ebbesen et al., Graphitic cones and the nucleation of curved carbon surfaces, *Nature (London)* **388**, 451 (1997).
- [57] S.N. Naess, A. Elgsaeter, G. Helgesen, K.D. Knudsen, Carbon nanocones: wall structure and morphology, *Sci. Tech. Adv. Mater.* **10**, 065002 (2009).
- [58] E.R. Bezerra de Mello, A.A. Saharian, Casimir effect in hemisphere capped tubes, *Int. J. Theor. Phys.* **55**, 1167 (2016).

- [59] S. Leizerovitch, B. Reznik, Charged particles in an external field: A QED analog with Bose-Einstein condensates, *Phys. Rev. A* **95**, 043611 (2017).
- [60] D. Musso, Simplest phonons and pseudo-phonons in field theory, *Eur. Phys. J. C* **79**, 986 (2019).
- [61] J. Jung, O. Keller, Bulk and surface plasmons: Wave-mechanical and second-quantized theories, *Phys. Rev. A* **103**, 063501 (2021).
- [62] *Handbook of Mathematical Functions*, edited by M. Abramowitz and I. A. Stegun (Dover, New York, 1972).
- [63] A. P. Prudnikov, Yu.A. Brychkov, O.I. Marichev, *Integrals and Series* (Gordon and Breach, New York, 1986), Vol. 2.
- [64] V.Kh. Kotanjyan, A.A. Sahariana, M.R. Setare, Vacuum currents in partially compactified Rindler spacetime with an application to cylindrical black holes, *Nucl. Phys. B* **980**, 115838 (2022).
- [65] P. Candelas, D.J. Raine, Quantum field theory on incomplete manifolds, *J. Math. Phys.* **17**, 2101 (1976).
- [66] G. N. Watson, *A Treatise on the Theory of Bessel Function* (Cambridge University Press, Cambridge, 1995).
- [67] F.W. Olver et al., *NIST Handbook of Mathematical Functions* (Cambridge University Press, USA, 2010).
- [68] S. Bellucci, A.A. Saharian, V. Vardanyan, Vacuum currents in braneworlds on AdS bulk with compact dimensions, *J. High Energy Phys.* **11** (2015) 092.
- [69] S. Bellucci, A.A. Saharian, V. Vardanyan, Hadamard function and the vacuum currents in braneworlds with compact dimensions: Two-brane geometry, *Phys. Rev. D* **93**, 084011 (2016).
- [70] S. Bellucci, A.A. Saharian, D.H. Simonyan, V.V. Vardanyan, Fermionic currents in topologically nontrivial braneworlds, *Phys. Rev. D* **98**, 085020 (2018).
- [71] S. Bellucci, A.A. Saharian, H.G. Sargsyan, V.V. Vardanyan, Fermionic vacuum currents in topologically nontrivial braneworlds: Two-brane geometry, *Phys. Rev. D* **101**, 045020 (2020).